Excess light priming in *Arabidopsis thaliana* with altered DNA methylomes

Bethany A. B. Stone*, Diep R. Ganguly*, Steven R. Eichten, Barry J. Pogson

Australian Research Council Centre of Excellence in Plant Energy Biology, Research School of Biology, The Australian National University Canberra, Acton, ACT, 0200, Australia.

*These authors contributed equally to this work.

Orcid IDs: BABS (0000-0003-3246-7943), DRG (0000-0001-6746-0181), SRE (0000-0003-2268-395X), BJP (0000-0003-1869-2423)

Corresponding author: Barry Pogson; barry.pogson@anu.edu.au

Author contributions: BABS, DRG, SRE, and BJP conceived and designed the study; BABS and DRG designed experiments; BABS performed the experimental work with guidance from DRG; BABS performed data analysis with guidance from DRG and SRE; BABS and DRG drafted the manuscript; all authors commented on and edited the manuscript.

One sentence summary: Photoprotection and priming against recurring excess light is functional despite impaired maintenance of the DNA methylome.

Short title: Excess light priming in *Arabidopsis* DNA methylation mutants

Keywords: DNA methylation, priming, gene expression, photoprotection.

Abstract

Plants must continuously react to the ever-fluctuating nature of their environment. Repeated exposure to stressful conditions can lead to priming, whereby prior encounters heighten a plant's ability to respond to future events. A clear example of priming is provided by the model plant species *Arabidopsis thaliana* (Arabidopsis), in which photosynthetic and photoprotective responses are enhanced following recurring light stress. While there are various post-translational mechanisms underpinning photoprotection, an unresolved question is the relative importance of transcriptional changes towards stress priming and, consequently, the potential contribution from DNA methylation – a heritable chemical modification of DNA capable of influencing gene expression. Here, we systematically investigate the potential molecular underpinnings of physiological priming against recurring excess light (EL), specifically DNA methylation and transcriptional regulation: the latter having not been examined with respect to EL priming. The capacity for physiological priming of photosynthetic and photoprotective parameters following a recurring EL treatment was not impaired in Arabidopsis mutants with perturbed establishment, maintenance, or removal of DNA methylation, nor was the transmission of this priming into naive tissues developed in the absence of excess light. Importantly, no differences in developmental or basal photoprotective capacity were identified in the mutants that may confound the above result. Little evidence for a causal transcriptional component of physiological priming was identified; in fact, most alterations in primed plants presented as a transcriptional 'dampening' in response to an additional EL exposure, likely a consequential of physiological priming. However, a set of transcripts uniquely regulated in primed plants provide preliminary evidence for a novel transcriptional component of recurring EL priming, independent of physiological changes. Thus, we propose that physiological priming of recurring EL in Arabidopsis occurs independently of DNA methylation; and that the majority of the associated transcriptional alterations are a consequence, not cause, of this physiological priming.

Introduction

Plants, as sessile organisms, must respond to various stresses imposed by their environment. Abiotic stresses may be long with unfavourable conditions persisting stably as characteristics of extreme climates. Alternatively, environments can be highly dynamic and comprise of transient, often recurring, stressful events. Information processing is key to efficient and effective physiological and developmental responses to specific environmental factors. Indeed, there is growing evidence that plants can ‘remember’ past experiences. In addition to long-term acclimation to sustained environmental changes, short-term plant stress responses are modified by prior exposure to a transient, and often recurring, specific environmental stimulus (referred to as priming). Here, the future fitness of a primed individual is increased by reducing the damage of stressful events, while the costs of initiating and maintaining priming are outweighed by the costs of stress exposure in an ‘un-primed’ state [1].

A variety of mechanisms have been reported to contribute towards stress priming including transcriptional memory underpinned by stalled RNA Pol II and elevated H3K4me3 [2], and fractionation of H3K27me3 patterns [3]. It has also been reported that the activity of the HSFA2 transcription factor can result in H3K4me2 and H3K4me3 changes, in response to recurring heat stress, resulting in transcriptional priming [4]. Additionally, HDA6-mediated histone H4 de-acetylation has been linked to prime jasmonic acid signalling leading to enhanced drought tolerance [5]. These various examples indicate that chromatin variation contributes towards plant stress priming. Another speculated chromatin mark to contribute towards stress priming is DNA methylation, variations in which, theoretically, could be stably inherited across mitotic cell divisions to convey persistent alterations in transcript expression [6]. The targeting of the RNA-directed DNA methylation (RdDM) pathway towards promoter regions of genes, and the occurrence of gene body methylation (gbM), suggests that differential methylation could arise within genes or their regulatory elements [7,8]. Such observations raise the potential regulatory capacity for DNA methylation.

An extant question is the exact regulatory potential of DNA methylation, which could affect stress responses. Canonically, DNA methylation is considered a mechanism for transcriptional repression, for example, through steric hindrance of RNA polymerase II [9]. This silencing is most pronounced at transposable elements (TEs) [10,11]. On the other hand, gbM is often found within constitutively expressed genes although there is conflicting evidence for an affect on transcription [7,12]. Other reports implicate the involvement of DNA methylation in alternative splicing and modulation of transcription factor binding capacity [13–15]. Given these various mechanisms, and placing DNA methylation in the broader context as being one of many chromatin modifications, it might be unsurprising that efforts to quantify the contribution of DNA methylation, at an organism level, towards transcription have shown a lacking relationship [16]. It has also been suggested that changes in the methylome may be a consequence of gene expression changes rather than a driver [17]. Trying to identify causative changes in the methylome is further complicated by the observation that effects of DNA methylation are not always observed in the adjacent gene [18].

Given these complications, various tools have been developed to quantify the effects of methylome variation on gene expression and physiological traits. The utilization of epigenetic recombinant inbred lines that display variable methylation patterns, but are genetically uniform, demonstrated that DNA methylation could contribute towards quantifiable phenotypic differences [19,20]. Mutants with defective methylation machinery that exhibit a variety of methylome variations, depending on the severity of the mutation, have also been used to correlate a relationship between DNA methylation and plant stress responses [21–23]. Mutants are also described to be developmentally or morphologically aberrant, however, it is not clear whether this is the direct result of methylation changes or an indirect effect of TE de-regulation and genome instability [24–27]. Indeed, traits attributed towards methylome variants could equally be tied to underlying TE activity [22,28,29].

We previously demonstrated that Arabidopsis is primed by a recurring EL regime, referred to as WLRS [30]. This priming was largely evident through altered non-photochemical quenching (NPQ) behaviour with improved photosystem II (PSII) efficiency. Despite the observation of physiological priming, we observed no associated changes in DNA methylation. While this demonstrated that the Arabidopsis methylome was impervious to recurring EL, it does not preclude the contribution of transcriptional regulation towards EL priming to which appropriate methylome maintenance may be important. In fact, enhanced induction of EL-responsive transcripts has been observed during systemic acquired acclimation (SAA), where EL-exposed tissues signal a state of enhanced responsiveness to unexposed systemic tissues conveying added protection [31–33]. As the methylation machinery was operational during previous analyses, any light-induced changes may have been reset prior to tissue harvesting. Indeed, the disruption of such machinery has revealed transgenerational effects that were otherwise reset [26,34,35]. Thus, we sought to clarify these unknowns by testing whether a range of mutants, unable to maintain their methylome, was capable of priming against recurring EL; and characterising the transcriptome of EL primed Col-0 plants. We report that first generation methylation mutants demonstrate functional photoprotection and EL priming, to a comparable extent as wild-type (WT) plants. Furthermore, whilst primed plants demonstrate a completely reset transcriptome they also displayed attenuated responses to further EL, which we refer to as “dampening”, potentially reflecting the reduced generation of signalling molecules due to enhanced photoprotection.

Results

Mutant characterisation and the novel *strs2* methylome

We utilized three Arabidopsis T-DNA insertion mutants targeting components of the DNA methylation machinery to test for stress priming with disrupted methylome maintenance. These include the triple methyltransferase mutant *drm1drm2cmt3* (*ddc3*) [36], the triple demethylase mutant *ros1dml2dml3* (*rdd*) [21], and the novel putative RdDM mutant *strs2* [37]. While the *ddc3* and *rdd* mutants show gross methylome changes across the genome, *strs2* displays subtle effects on the methylome by fine-tuning DNA methylation levels at stress-associated genes [37].

As previous studies investigating *strs2* relied on a targeted analysis using chop-PCR, we performed MethylC-seq (n=3) to confirm the extent of methylome changes. Global levels of CG, CHG, and CHH methylation in *strs2* were highly comparable to WT (Figure 1 A, Supplementary Dataset 1). However, employing *DSS* to identify differentially methylated regions (DMRs) revealed moderate levels of local changes, predominantly in the CG context, with comparable numbers of hyper- and hypo-DMRs (Figure 1 B, Table 1, Supplementary Dataset 2). Nonetheless, many CHH DMRs were located within TEs consistent with the implication of STRS2 in RdDM. Furthermore, 130/199 (65.6%) *strs2* CHH hypo-DMRs were regions targeted by DRM1 and DRM2 (7,393 CHH hypo-DMRs in *drm1drm2*), whereas CG and CHG hypo-DMRs demonstrated weaker overlaps (CG: 7/318, 2.2%; CHG: 8/34, 23.5%). Paired with previous results this suggests that *strs2* is a “weak” RdDM mutant [38].

Development and basal photoprotection of methylome mutants

Aberrant DNA methylation is considered to result in developmental differences due to transcriptional misregulation and TE activation; *ddc3* displays curled leaves and reduced stature due to *SDC* misexpression [36], while *strs2* shows a slight early flowering phenotype [39]. To ensure that developmental abnormalities would not confound observations of priming, developmental traits were monitored until 4-weeks of age starting from 10-day old seedlings (Figure 2). While no unusual phenotypes were evident for *rdd* and *strs2* (Figure 2 A), *ddc3* displayed the expected curled leaves from 3-weeks of age. Quantitative measures of plant area reflect these visible observations, whereby the rosette area of *ddc3* was reduced compared to WT (Figure 2 B). Minor differences in leaf number and plant area were observed in 3-week old *rdd* and *strs2*, though are subtle compared to *ddc3*. Importantly, the above abnormalities presented after 21 days, and thus are unlikely to confound observations of priming (measured in plants 3-weeks of age).

In addition to developmental abnormalities, aberrant methylome maintenance may also affect the capacity for basal photoprotective responses. Thus, functional PSII capacity was tested in 3-week old mutants (Figure 2 C). Photosynthetic efficiency (ΦPSII) was largely consistent across genotypes. Similarly, the capacity for, or activation of, actively regulated (ΦNPQ) and constitutively (ΦNO) dissipative quenching was largely consistent across genotypes. An exception to this was *rdd* that demonstrated elevated ΦNPQ with a concomitant reduction in ΦNO but unperturbed ΦPSII. However, the difference observed in *rdd* is minor compared to traditional mutants with truly perturbed photosystems [40] and is more reflective of natural variation [41]. Thus, no major disruptions to basal PSII performance is evident in these methylation mutants allowing for comparisons of EL priming.

Excess light priming evident despite aberrant methylome patterning

To investigate whether a perturbed methylome would impair priming to recurring EL we repeated the WLRS time-course experiment [30] on WT, *ddc3*, *rdd*, and *strs2* (Figure 3). The week of recurring EL led to the expected morphological differences across all genotypes, namely increased rosette compaction but consistent leaf area (Figure 3 A-B). However, there was an attenuated difference in *ddc3* area, which we attribute to its naturally curled leaf

phenotype. Alongside morphological measures were changes in PSII traits indicative of physiological priming to recurring EL (Figure 3 C). The adoption of ΦNPQ and ΦNO also revealed distinct patterns in thermal dissipation not observed previously. Particularly, that the enhanced NPQ was underpinned by actively regulated pH-dependent thermal dissipation (ΦNPQ) rather than due to constitutive forms (ΦNO). Indeed, ΦNO was lower in primed plants. While ΦNPQ is rapidly activated in primed plants, it is deactivated concomitantly with an increase in ΦPSII. A key result here was that all methylation mutants demonstrated a WT-like priming response, for all three PSII traits, to recurring EL thus demonstrating appropriate light-acclimatory processes despite having perturbed methylomes.

Primed plants exhibit transcriptional 'dampening' despite a reset transcriptome

Persistent changes in gene expression are hypothesized to convey a primed state [1]. To test this, we searched for constitutive changes in gene expression between naive and primed plants (N vs P, n=3) after one-week of recurring EL using mRNA-seq. Despite the observation of physiological priming in these tissues, we observed a completely reset transcriptome exemplified by poor separation of N and P libraries and identifying 0 DEGs (Figure S1 A-B). We subsequently investigated the transcriptional response of primed plants to an additional EL treatment (triggering stress, P+T). As expected, application of an EL triggering stress to naive plants (N+T) elicited the differential expression of hundreds of genes, however, primed plants showed a vastly attenuated response (Figure S1 C-D, Supplementary Datasets 4 - 5). While the majority of EL-induced transcripts in P+T plants overlapped with those in N+T plants, a striking proportion of both up- and down-regulated transcripts were unique to N+T plants (Figure 4 A). The abundance of nearly all 318 uniquely down-regulated transcripts in N+T plants was greater in P+T plants (Figure 4 B, left). Conversely, abundance of the 256 uniquely up-regulated transcripts in N+T plants was decreased in P+T plants (Figure 4 B, right). Together, these results suggest a dampened transcriptional response to EL triggering stimuli in primed plants, rather than reflecting differences between their basal (un-triggered) transcriptomes. The dampening effect is, however, subtle in nature - no DEGs were identified upon direct comparison of N+T and P+T samples.

A variety of signalling molecules, such as reactive oxygen species (ROS), are generated by EL and are responsible for the induction of EL-responsive genes to promote oxidative stress tolerance [32,42,43]. Thus, we hypothesised that the transcriptional dampening observed in primed plants may be a consequence of reduced signalling because of enhanced dissipative quenching (e.g. lesser ROS production). Indeed, a gene ontology analysis of all 574 transcripts exhibiting dampening (Supplementary Dataset 6), in primed plants, revealed an enrichment for terms associated with response to abiotic stimuli, including light intensity, as well as response to ROS and hydrogen peroxide, supporting this hypothesis (Supplementary Dataset 7). Genes induced by various ROS (hydrogen peroxide [H_2O_2], singlet oxygen [$^1O_2$], and superoxide [O^{2-}] [44]), salicylic acid (SA) [45], β-cyclocitral [46], ABA [47], and SAA [32] were overlapped with the dampened transcripts identified here. In total, 198/574 (34.5%, $P_{[X\geq198]} < 0.05$) dampened transcripts were overlapped from the collated gene list. This was driven by significant overlaps

with ABA, β-Cyclocitral, and SAA induced genes as determined by hypergeometric testing (Table 2). Thus, dampening of triggered transcripts in primed plants may reflect reduced levels of EL induced signals as a result of improved photochemical efficiency.

Discussion

The popular notion that DNA methylation may regulate plant stress responses is confounded by both supporting and conflicting investigations spanning a range of plant species and stress types. Light stress is one such example for which physiological priming and memory have been demonstrated in Arabidopsis, yet no co-occurring stress-induced DNA methylation changes are observed [30,33,48]. This study builds on these findings, but addresses a distinct hypothesis: that physiological priming of recurring EL is underpinned by transcriptional regulation, for which active maintenance of DNA methylation is important. Here, evidence for recurring EL priming is combined with examples of perturbed stress responses in DNA methylation mutants, using a full-factorial experimental design that has allowed systematic testing of two closely related potential priming mechanisms: 1. DNA methylation-mediated transcriptional regulation; and 2. altered transcription (independent of DNA methylation).

DNA methylation, development, and priming

The mechanisms by which DNA methylation could contribute to phenotypic variation remains an outstanding question [49]. One potential is for targeted DNA methylation and gene silencing via the RdDM pathway [8]. For example, a link between the function of DEAD-box RNA helicase STRS2 in attenuating abiotic stress responses via RdDM has previously been suggested [37]. Here, we profile the exact nature of methylation changes in *strs2* and consider it to represent a “weak” RdDM mutant, affecting only a small portion of RdDM-targeted regions. Conversely, STRS2 appears to be more important for CG methylation suggestive of a role beyond RdDM. The exact molecular function of STRS2 is yet to be confirmed, however, cellular mis-localisation of STRS2 in upstream RdDM mutants implicates a role in siRNA biogenesis [37]. Furthermore, in this study, no abiotic stress treatment was applied to *strs2* prior to MethylC-seq. Thus, alterations to DNA methylation required for post-stress gene silencing would not have been captured. Regardless, the relatively subtle and targeted nature of *strs2* complemented the use of the more severe and widespread methylome effects in *rdd* and *ddc3* [10].

DNA methylation is considered to be required for appropriate plant physiology by maintaining genome integrity and patterns of gene expression [10]. However, it is unclear whether these effects are a direct result of perturbed methylomes or an indirect effect over generations of compromised genome integrity [26]. Through detailed observation of first generation mutants, we find negligible developmental aberrations that might be directly tied to methylation changes besides the previously reported curled leaf morphology of *ddc3* [36]. These results align with the view that loss of active methylome maintenance manifests into aberrant development over generations of compromised genome stability as opposed to methylation-dependent transcriptional control.

Light acclimation involves multiple levels of regulatory changes [50]. Indeed, the importance of transcriptional control should not be underestimated, for example, regulation of chloroplast development [51], photooxidative stress tolerance [32], or chloroplast-mediated thermotolerance [52]. Since light-induced gene expression changes contribute towards light acclimation [32,50,53,54], it was hypothesized that changes in DNA methylation might impact appropriate transcriptional control thus impairing the ability for EL priming. Contradictory to this, perturbation of the methylome, regardless of severity or type (hyper- or hypo-methylation), did not impair basal photoprotective capacity nor the ability to be primed by recurring EL. Instead, the EL priming observed herein likely reflects post-transcriptional changes of the photosynthetic machinery. For example, a reduction in levels of PSII supercomplexes and functional PSII antenna size has been correlated to growth under high light intensity [55]. The reduction in ΦNO disputes constitutive changes in PSII conformation. Rather there appears to be increased electron flow in primed plants, indicated by increased ΦPSII, which may reflect an increased concentration of components facilitating photosynthetic electron transport, such as PSII core proteins, cytochrome b_6f, and chloroplastic ATPases [56–58]. Irrespective of the exact mechanism, pertinent to this study is the observation that these processes remain functional under a range of methylome perturbations. One caveat here is that the exact transcriptional control conveyed by DNA methylation is unclear [16,17] and a complementary strategy, for example using transcriptional shut-off experiments, may provide greater evidence for the importance of transcriptional regulation towards EL priming.

Priming occurs independently of transcriptional changes

Persistent transcriptional up-regulation of light-responsive genes is often used as a marker for light acclimated leaves, however, it remains an untested hypothesis whether this priming may be underpinned by persistent transcriptional alterations. No persistent changes in gene expression were observed in primed plants, consistent with previous reports of rapid transcriptome resetting following EL treatment [59]. Altered transcript responsiveness was instead observed in primed plants responding to a final triggering stress, characterised by an attenuated response (“transcriptional dampening”). This contrasts the expected enhanced transcriptional response often observed following repeated EL [32,33,43,59]. Instead, an attenuated transcription response likely reflects a greater capacity to deal with increased light flux on primed plants.

Enhanced photosynthetic and photoprotective capacity in primed plants may alter levels of signalling molecules produced by EL. Changes in the rate of electron flow through the photosynthetic apparatus and chloroplast state alters these signals to modify nuclear gene expression. For instance, chloroplast regulation of nuclear gene expression under EL was impaired by disrupting effective photosynthetic electron flow, leading to PSI photodamage and the attenuation of oxylipin biosynthesis and signalling [60]. Furthermore, impairing photosynthetic electron flow, thus disrupting the state of the plastoquinone pool, attenuates transcriptional responses required for thermal acclimation [52]. Taken together, it was hypothesized that the dampened transcriptional response might be a consequence of altered signalling as a result of physiological priming. In support of this hypothesis was the observation that approximately one-third of dampened transcripts overlapped with genes induced by

signalling pathways, especially ABA, β-Cyclocitral, and SAA. On the other hand, two-thirds of dampened transcripts were not accounted for from this analysis and levels of these signalling molecules were not assayed directly. Thus, it remains speculative as to the exact cause of the dampened effect. Nonetheless, these results suggest that the gene expression changes observed in primed plants are consequential of physiological priming, rather than the cause.

Conclusion

Through the analysis of Arabidopsis mutants impaired in active methylome maintenance, we have conducted a systematic investigation of the notion that DNA methylation may contribute to stress priming, specifically addressing the hypothesis that physiological priming of recurring EL is underpinned by transcriptional regulation and active methylome maintenance. We found no evidence to suggest that aberrant maintenance or removal of DNA methylation impaired the capacity for physiological priming against recurring EL. In fact, primed plants demonstrated completely reset transcriptomes. Instead, an attenuation in transcriptional response to EL was observed in primed plants, likely a consequence of priming.

Methods

Plant growth and germplasm

All *Arabidopsis* germplasm utilized were in the Columbia (Col-0) background. Plant lines comprised of wild-type Col-0 (WT), the DNA methylation establishment triple mutant *ddc3* (CS16384; *drm1*-2 *drm2*-2 *cmt3*-11), the “weak” RdDM mutant *strs2* (SALK_028850), and the triple demethylase mutant *rdd* (derived from *ros1-4,* SALK_045303; *dml2,* SALK_131712; *dml3-2*, SALK_056440). All seeds were obtained from the Arabidopsis Biological Research Centre (Ohio State University, Columbus, OH, USA), with the exception of *rdd* which was kindly provided by Dr. Ming-Bo Wang (CSIRO, Canberra, Australia) [21]. Second generation *ddc3*, *rdd*, and *strs2* were studied. Primers used for genotyping are listed in Supplementary Dataset 8.

For plant growth, Arabidopsis seeds were sown onto individual pots containing moist Seed Raising Mix (Debco, NSW, Australia). Soil was supplemented with Osmocote Exact Mini slow release fertilizer (Scotts, NSW, Australia) at a concentration of 1 g/L dry volume of soil and treated with 1 L of 0.3 % (v/v) AzaMax (OCP, NSW, Australia) prior to sowing to prevent insect infection. Seeds were covered with clear plastic wrap and stratified at 4°C in the dark for at least 72 hours to break dormancy and coordinate germination. Stratified seeds were transferred to a temperature controlled Conviron S10H growth chamber (Conviron, Winnipeg, MB, Canada) for cultivation under standard growth conditions: 12-hour photoperiod (08:00-20:00), 100-150 µ mol photons m^{-2} s^{-1}, 20 °C (± 2 °C), 55% (± 5 %) relative humidity. Upon germination, clear plastic wrap was slowly removed over 7-10 days, to maintain high humidity until seedlings were well-established and to avoid humidity shock. Plants were watered every 2-3 days depending on soil moisture, avoiding pooling of water to prevent algal and fungal growth. Each of three daily EL treatments consisted of 60 minutes of 1000 µ mol photons m^{-2} s^{-1} using a mixture of metal halide and high-pressure sodium lamps as previously described [30,59].

For MethylC- and mRNA-seq experiments, developmentally equivalent leaves were harvested for comparisons (true leaves 4 - 9 in order of emergence). Harvested tissue was flash-frozen in liquid N_2 and ground into a fine powder using a 1/8″ steel ball bearing, in a 1.5 ml Eppendorf tube, with 1 min shaking at 25 Hz in the *Tissue Lyser II* (Qiagen, Hilden, Germany). Ground tissue was stored at -80 °C. Approximately 20 and 30 mg of ground tissue was used for extracting total RNA and genomic DNA, respectively. MethylC-seq of WT and *strs2* was performed on paired tissue samples by using aliquots of ground frozen tissue from the same harvested plant.

High-Throughput Phenotyping

For all genotypes the development of 10-day old (post-germination) Arabidopsis seedlings was followed for 20 days (until 4-weeks of age) by measuring plant area and rosette compactness. The *PlantScreen Compact System* (Photon Systems Instruments, Brno, Czech Republic), a high-throughput platform for digital plant phenotyping, was used to measure plant area and rosette compactness at 08:00 daily. Images were analysed using the *PSI RGB-IR Analyzer* software (version 1.0.0.2; Photon Systems Instruments, Brno, Czech Republic). Program settings were adjusted as needed to achieve well-defined plant areas and minimise background noise. The total number of macroscopically visible true leaves (cotyledons excluded) per rosette were also manually counted daily.

Monitoring PSII performance using chlorophyll fluorescence measurements

PSII photochemistry was probed in vivo using measures of chlorophyll fluorescence [61] using a PSI FluorCam (Photon System Instruments; Brno, Czech Republic). Measures were taken between 11:00-14:00 across the adaxial side of 30 minute dark adapted rosettes as performed previously [30]. In this study, intermittent measures of chlorophyll fluorescence, specifically F_t, F_m, and F_m', were taken after a saturating pulse (3000 µ mol photons m^{-2} sec^{-1}) across 10-minutes in actinic light (700 µ mol photons m^{-2} sec^{-1}) followed by a 4-minute dark period (https://goo.gl/RuYDE2). The resulting fluorescence images were analysed using the FluorCam 7 software (v1.1.1.4; Photon System Instruments, Brno, Czech Republic). Chlorophyll fluorescence signals were analysed across whole rosettes. To better quantify light energy partitioning between photochemistry, light-regulated thermal dissipation, and other non-light induced quenching, such as chlorophyll fluorescence, we adopted the yield terms of ΦPSII, ΦNPQ, and ΦNO (Table 3), which sum to unity and do not require measures of F_o [62,63].

MethylC sequencing

Genomic DNA was extracted from ground tissue using the *DNeasy Plant Mini Kit* (Qiagen, Netherlands) according to the manufacturer's instructions, and quantified using a *ND-1000* Spectrophotometer. 70 ng of *Covaris* sheared gDNA (average fragment size = 200 bp) was bisulfite converted using the *EZ DNA Methylation-Gold Kit* (Zymo Research, CA, USA) according to the manufacturer's instructions. Bisulfite converted DNA was used to create dual-indexed MethylC-seq libraries using the *Accel-NGS Methyl-Seq DNA Library Kit* paired with the

Accel-NGS Methyl-Seq Dual Indexing Kit (Swift Biosciences, MI, USA) according to manufacturer' instructions. All libraries were amplified in a 7-cycle indexing PCR reaction. All clean-ups were performed using either *AMPure XP beads* (Beckman Coulter, CA, USA) or *Sera-mag SpeedBeads* (GE Healthcare, Buckinghamshire, UK). A *LabChip GXII* (Perkin Elmer, MA, USA) was used to determine library molarity and fragment size distribution. Libraries were pooled in equimolar ratios and sequenced on one HiSeq2500 flow cell (100 bp single-end) at the *ACRF Biomolecular Research Facility* (Australian National University, ACT, Australia). In-depth details of library preparation are also described on protocols.io (https://goo.gl/vfwtEU).

Raw reads were quality controlled using *FastQC* (v0.11.2) with reads filtered and trimmed using *Cutadapt* (v1.9) and *Trim Galore!* (v.0.3.7) under default parameters. Single-end alignments of trimmed raw reads were aligned to the TAIR10 reference using *Bismark* (v0.14.5) [64] and *Bowtie2* (v2.2.9) [65] with the flags -N 0 and -L 20. Per cytosine methylation levels were calculated using *Bismark methylation extractor* with default settings. Only cytosines with read depth > 3X were retained for further analysis. Bisulfite conversion efficiency was calculated as the proportion of methylated cytosines in the CHH context within the chloroplast genome, which itself should be fully unmethylated. Alignment metrics are provided in Supplementary Dataset 1. Weighted methylation levels were used to calculate the proportion of CG, CHG, and CHH methylation to account for sequencing depth [66]. This output was binned into 50 kbp regions (filtered for read depth > 15X) across the genome to construct chromosomal level metaplots of methylation levels using *BEDTools [67]*

Weighted methylation levels at single cytosines was utilized in DMR identification using *DSS* (v2.28.0) with default settings, including smoothing (*smoothing span* = 100) to improve methylation estimates [68,69]. Differentially methylated cytosines (DMCs) were called (*DMLtest*) based on the posterior probabilities (q-value < 0.05) for a threshold in methylation difference (delta) at each cytosine in a context-specific manner: 0.5 CG, 0.2 CHG, and 0.1 CHH. Subsequently, DMRs are called based on adjacent statistically significant DMCs (*callDMR* with default parameters). These were refined by removing regions with a merged test statistic (*areaStat*) and estimated methylation difference in the lowest quartile, per sequence context, to remove DMRs containing DMCs of opposite direction. The final list of DMRs were assigned genomic positions, or overlapped between comparisons, using *BEDTools* and the *Araport11* annotation [67,70]. Code used for analyses are available on Github (https://goo.gl/wsQrJT).

Independent WT and *drm1drm2* MethylC-seq profiling was accessed from GSE39901 and GSE38286. DRM1/2-dependent RdDM sites were determined as the CHH hypo-DMRs identified in common between *drm1drm2* and three independent WT samples using *DSS* with same parameters used herein [38].

mRNA sequencing

Total RNA was extracted with *TRIzol* (Life Technologies) using an adapted protocol [71]. Briefly, ground tissue was lysed in 1 ml *TRIzol* and mixed by gentle inversion and incubated at room temperature for 5 minutes. Subsequently, 200 µl chloroform was added and shaken vigorously to mix. Samples were centrifuged at 14,000 rcf for 10 min at 4°C to separate the resulting upper

aqueous phase from the organic phase. Chloroform extraction was repeated twice, transferring 400-600 µl then 300-400 µl aqueous phase to a new microfuge tube following each extraction. RNA was precipitated by adding equal volume of 100% isopropanol and mixing by inversion before incubating at -20°C overnight. RNA was recovered by 4°C centrifugation at 20,000 rcf for 20 min, the supernatant discarded, and pellet washed with 80% ethanol and centrifuged at 7,500 rcf for a further 3 min. The supernatant was discarded and the pellet air-dried prior to resuspension in 50 µl DEPC-treated H_2O. All purified RNA was stored at -80°C. RNA quantity was assessed using *ND-1000 spectrophotometer* (NanoDrop Technologies). RNA quality was assessed using the *LabChip GXII* (Perkin-Elmer) for RIN > 6.5.

Poly(A)-enriched RNA-sequencing (mRNA-seq) libraries were prepared using the *Illumina TruSeq Stranded mRNA Sample Preparation Kit* (Illumina, CA, USA) using 1.3 µg input of extracted total RNA. The following modifications to the manufacturer's instructions were made: reagent volumes were adjusted for 1/3 reactions; and Invitrogen SuperScript III Reverse Transcriptase (Invitrogen, Life Technologies Australia Pty Ltd) was used for first strand synthesis with adjusted reaction temperature of 50 °C. Libraries were constructed using *Illumina TruSeq RNA Single Indexes* (Set A and B; Illumina, CA, USA) in a 14-cycle indexing PCR reaction; all clean-ups were performed using *RNAClean XP beads* (Beckman Coulter, CA, USA). A *LabChip GXII* (Perkin Elmer, MA, USA) was used to determine library concentration and fragment size distribution, using a DNA High Sensitivity Kit. mRNA-seq libraries were pooled in equal molar ratios and sequenced (75 bp single-end) on one lane of a *NextSeq500* at the ACRF Biomolecular Research Facility (Australian National University, ACT, Australia).

Raw reads were diagnosed using *FastQC* (v0.11.2). Due to strong nucleotide sequence content bias *Trim Galore!* and *Cutadapt* were used to trim low-quality reads with PHRED score < 20 (-q 20) and to make a hard clip of 10 bp and 1 bp from the 5' and 3' ends, respectively. Single-end alignments of trimmed raw reads were aligned to the *TAIR10* reference genome using *Subread* (v1.6.2) [72] with the flags -t 0 and -u to report uniquely mapping reads, prior to sorting, indexing and compressing using *Samtools* (v1.2). Alignment metrics are provided Supplementary Dataset 3. Transcript quantification was performed at the gene-level with the *Araport11* annotation [70] using *featureCounts* (with flag -s 2 for reverse strand specificity).

Differential gene expression analyses were performed using the *edgeR* quasi-likelihood pipeline [73]. Reads mapping to ribosomal RNA and organellar transcripts were removed; only loci containing counts per million (CPM) > 1 in at least three samples were examined. After this filtering, 17,657 loci were retained for analysis. The trimmed mean of M-values (TMM) method was used to normalise transcript abundance between libraries to account for sequencing depth and composition. Subsequently, generalised linear models were fitted to estimate dispersion (*glmQLFit*) allowing for differential expression testing, employing quasi-likelihood F-tests (*glmQLTest*) and controlling for false discovery rates due to multiple hypothesis testing (FDR adjusted p-value < 0.05). Gene ontology enrichments were examined using the *statistical overrepresentation test* (Binomial test with FDR correction) from the PANTHER classification suite [74]. Code used for RNA-seq analyses are available on Github (https://goo.gl/b7x5rc).

Statistical analyses

Statistical analyses and data visualisation was performed using *R* (v 3.5.0) with the *tidyverse* package (v 1.2.1). Linear mixed-effects models were fitted using the *lme4* package (v 1.1-17 [75]) to account for both fixed (e.g. genotype, condition, time) and random effects (e.g. experimental design, blocking factors). Model fit was assessed using the conditional R^2 value calculated using the *piecewiseSEM* package (v 2.0.2 [76]). Fitted models allowed estimation of marginal means and 95% confidence intervals using the *emmeans* package including *post hoc* contrasts between factors with FDR p-value correction (v 1.2.1). All analyses were performed on single data points, representing individual biological replicates (independent plants). Hypergeometric testing was performed using the *phyper* function to test for significant overlaps, taking into account the background 17,657 total detected transcripts and the number of stress signalling-associated genes overlapped.

Data accessibility

All sequencing data generated for this study has been deposited at the NCBI GEO repository: GSE121150.

Supplemental Datasets

Supplementary Dataset 1 MethylC-seq statistics
Supplementary Dataset 2 *strs2* DMRs
Supplementary Dataset 3 RNA-seq statistics
Supplementary Dataset 4 Differentially expressed genes following triggering stress in naive plants
Supplementary Dataset 5 Differentially expressed genes following triggering stress in primed plants
Supplementary Dataset 6 Dampened transcripts
Supplementary Dataset 7 Enriched GO terms among dampened transcripts
Supplementary Dataset 8 Genotyping primers

Acknowledgements

We would like to acknowledge the advice received from Prof. Wah Soon Chow on chlorophyll fluorescence based measures of photosynthetic performance. We would also like to acknowledge the Biomolecular Resource Facility at the ANU for performing Illumina sequencing, and Dr Terry Neeman for advice on statistical analyses. This project was also supported with the provision of plant growth facilities by the Australian Plant Phenomics Facility and computational infrastructure by the National Computational Infrastructure, both supported under the National Collaborative Research Infrastructure Strategy of the Australian Government.

This project was funded by the Australian Research Council Centre of Excellence in Plant Energy Biology (CE140100008). DRG was supported by the Grains Research and Development

Council (GRS10683) and an Australian Research Training Program (RTP) Scholarship. SRE. was funded by a Discovery Early Career Researcher Award (DE150101206).

The authors declare no conflicts of interest.

Tables

Table 1 DMR analysis in *strs2* (vs WT)

DMR type	Methylation context			
	CG	CHG	CHH	Total
Hyper-methylation	700	68	148	916
Hypo-methylation	684	38	226	948
Total	1,384	106	374	1,864

Table 2 Hypergeometric testing of 574 dampened transcripts overlapped with genes involved in stress signalling

Gene list	**Total responsive genes**	**Overlap with dampened transcripts**	**Hypergeometric test**
ABA	2,481	104	$P_{[X\geq104]} < 0.01$
SA	217	7	$P_{[X\geq7]} = 0.56$
O_2^-	209	5	$P_{[X\geq5]} = 0.81$
H_2O_2	325	11	$P_{[X\geq11]} = 0.49$
$^1O_2$	295	10	$P_{[X\geq10]} = 0.49$
β-Cyclocitral	1,145	61	$P_{[X\geq61]} < 0.001$
SAA	703	41	$P_{[X\geq41]} < 0.001$

Table 3 Diagnostic PSII parameters and their biological relevance

Parameter	Equation	Interpretation
ΦPSII	$1 - F_t/F_m'$	Fraction of light absorbed by PSII for photochemistry.
ΦNPQ	$F_t/F_m' - F_t/F_m'$	Fraction of light absorbed by PSII that is lost via thermal dissipation (ΔpH- and xanthophyll-regulated processes).
ΦNPQ	F_t/F_m	Fraction of light absorbed by PSII that is lost via chlorophyll fluorescence.

Figure legends

Figure 1 Subtle methylome perturbation in *strs2*
A Mean weighted methylation levels, binned into 50 kbp rolling windows, along Arabidopsis chromosome 1 for WT and *strs2*.
B DMR frequency in *strs2* grouped by genomic location relative to annotated genes or transposable elements. DMRs were classified as either occurring directly within (body), <1 kbp away from the 5` (upstream) or 3`end of (downstream), or > 1 kbp (intergenic) away from genomic features.

Figure 2 DNA methylation mutant development and basal PSII function
A Representative morphology of WT, *ddc3*, *rdd*, and *strs2* from 2-4 weeks of age.
B Leaf number (left) and plant area (right) in 10-day old WT (red, n=8), *ddc3* (purple, n=8), *rdd* (orange, n=8), and *strs2* (green, n=8) seedlings, monitored for 20 days until 4-weeks of age.
C Measures of PSII performance in 3-week old WT (red, n=60), *ddc3* (purple, n=10), *rdd* (orange, n=10), *strs2* (green, n=15) plants grown under standard conditions.
Points denote estimated marginal means based on a fitted linear mixed-effect model for each genotype. Bars and shaded regions denote 95% confidence intervals; * indicates statistical significance (adjusted p-value<0.05) from WT.

Figure 3 DNA methylation mutants exhibit priming to recurring EL
A-B Boxplots of rosette area and compactness measured in all genotypes either exposed to recurring EL (primed, n=12-15) or not (naive, 21-23). * denotes statistical significance determined using independent Student's t-tests for each genotype (adjusted p-value < 0.05).
C PSII performance traits in naive (WT n=22; *ddc3* n=16, *rdd* n=21, *strs2* n=23) and primed (WT n=16; *ddc3* n=13, *rdd* n=12, *strs2* n=15) plants for all genotypes. Points denote estimated marginal means based on a fitted linear mixed-effect model for each genotype. Bars and shading denote 95% confidence intervals; * indicates statistical significance (adjusted p-value < 0.05) from WT.

Figure 4 Transcriptional 'dampening' evident in EL primed plants
A Overlap between up- and down-regulated transcripts in naive and primed plants in response to an additional triggering EL treatment.

B Transcript abundance (log_2 RPKM) of up- (left) and down-regulated (right) transcripts, in N+T plants, for both N+T and P+T plants.
C Identifying dampened transcripts that are inducible by various stress signals. * denotes significant overlaps ($p<0.05$) as determined by a hypergeometric test using *phyper*.

Figure S1 Exploratory transcriptome analysis of naive and primed plants
A Multi-dimensional scaling plot of all samples where distance reflects the typical log_2 fold change between samples.
B-D Mean-difference plots for **B** primed versus naive libraries, **C** naive-triggered versus naive libraries, and **D** primed-triggered versus primed libraries with smearing of low abundance transcripts. Each dot represents a transcript plotted by its average abundance (log_2 CPM) against the log_2 fold change from the specified comparison. Red dots indicate differentially expressed transcripts as determined by quasi-likelihood F-tests (FDR < 0.05). Blue lines denote 2-fold change.

Bibliography

[1] M. Hilker, J. Schwachtje, M. Baier, S. Balazadeh, I. Bäurle, S. Geiselhardt, D.K. Hincha, R. Kunze, B. Mueller-Roeber, M.C. Rillig, J. Rolff, T. Romeis, T. Schmülling, A. Steppuhn, J. van Dongen, S.J. Whitcomb, S. Wurst, E. Zuther, J. Kopka, Priming and memory of stress responses in organisms lacking a nervous system, Biol. Rev. Camb. Philos. Soc. 91 (2016) 1118–1133.

[2] Y. Ding, M. Fromm, Z. Avramova, Multiple exposures to drought “train” transcriptional responses in Arabidopsis, Nat. Commun. 3 (2012) 740.

[3] E. Sani, P. Herzyk, G. Perrella, V. Colot, A. Amtmann, Hyperosmotic priming of Arabidopsis seedlings establishes a long-term somatic memory accompanied by specific changes of the epigenome, Genome Biol. 14 (2013) R59.

[4] J. Lämke, K. Brzezinka, S. Altmann, I. Bäurle, A hit-and-run heat shock factor governs sustained histone methylation and transcriptional stress memory, EMBO J. 35 (2016) 162–175.

[5] J.-M. Kim, T.K. To, A. Matsui, K. Tanoi, N.I. Kobayashi, F. Matsuda, Y. Habu, D. Ogawa, T. Sakamoto, S. Matsunaga, K. Bashir, S. Rasheed, M. Ando, H. Takeda, K. Kawaura, M. Kusano, A. Fukushima, T.A. Endo, T. Kuromori, J. Ishida, T. Morosawa, M. Tanaka, C. Torii, Y. Takebayashi, H. Sakakibara, Y. Ogihara, K. Saito, K. Shinozaki, A. Devoto, M. Seki, Acetate-mediated novel survival strategy against drought in plants, Nat Plants. 3 (2017) 17097.

[6] P.A. Crisp, D. Ganguly, S.R. Eichten, J.O. Borevitz, B.J. Pogson, Reconsidering plant memory: Intersections between stress recovery, RNA turnover, and epigenetics, Sci Adv. 2 (2016) e1501340.

[7] A.J. Bewick, L. Ji, C.E. Niederhuth, E.-M. Willing, B.T. Hofmeister, X. Shi, L. Wang, Z. Lu, N.A. Rohr, B. Hartwig, C. Kiefer, R.B. Deal, J. Schmutz, J. Grimwood, H. Stroud, S.E. Jacobsen, K. Schneeberger, X. Zhang, R.J. Schmitz, On the origin and evolutionary consequences of gene body DNA methylation, Proc. Natl. Acad. Sci. U. S. A. 113 (2016) 9111–9116.

[8] M.A. Matzke, R.A. Mosher, RNA-directed DNA methylation: an epigenetic pathway of increasing complexity, Nat. Rev. Genet. 15 (2014) 394–408.

[9] P.L. Molloy, Effects of DNA methylation on specific transcription by RNA polymerase II in vitro, Mol. Biol. Rep. 11 (1986) 13–17.
[10] R. Lister, R.C. O'Malley, J. Tonti-Filippini, B.D. Gregory, C.C. Berry, A.H. Millar, J.R. Ecker, Highly integrated single-base resolution maps of the epigenome in Arabidopsis, Cell. 133 (2008) 523–536.
[11] S.J. Cokus, S. Feng, X. Zhang, Z. Chen, B. Merriman, C.D. Haudenschild, S. Pradhan, S.F. Nelson, M. Pellegrini, S.E. Jacobsen, Shotgun bisulphite sequencing of the Arabidopsis genome reveals DNA methylation patterning, Nature. 452 (2008) 215–219.
[12] A. Muyle, B.S. Gaut, Loss of gene body methylation in Eutrema salsugineum is associated with reduced gene expression, Mol. Biol. Evol. (2018). doi:10.1093/molbev/msy204.
[13] Y. Yin, E. Morgunova, A. Jolma, E. Kaasinen, B. Sahu, S. Khund-Sayeed, P.K. Das, T. Kivioja, K. Dave, F. Zhong, K.R. Nitta, M. Taipale, A. Popov, P.A. Ginno, S. Domcke, J. Yan, D. Schübeler, C. Vinson, J. Taipale, Impact of cytosine methylation on DNA binding specificities of human transcription factors, Science. 356 (2017). doi:10.1126/science.aaj2239.
[14] R.C. O'Malley, S.-S.C. Huang, L. Song, M.G. Lewsey, A. Bartlett, J.R. Nery, M. Galli, A. Gallavotti, J.R. Ecker, Cistrome and Epicistrome Features Shape the Regulatory DNA Landscape, Cell. 165 (2016) 1280–1292.
[15] S. Shukla, E. Kavak, M. Gregory, M. Imashimizu, B. Shutinoski, M. Kashlev, P. Oberdoerffer, R. Sandberg, S. Oberdoerffer, CTCF-promoted RNA polymerase II pausing links DNA methylation to splicing, Nature. 479 (2011) 74–79.
[16] D. Meng, M. Dubin, P. Zhang, E.J. Osborne, O. Stegle, R.M. Clark, M. Nordborg, Limited Contribution of DNA Methylation Variation to Expression Regulation in Arabidopsis thaliana, PLoS Genet. 12 (2016) e1006141.
[17] D. Secco, C. Wang, H. Shou, M.D. Schultz, S. Chiarenza, L. Nussaume, J.R. Ecker, J. Whelan, R. Lister, Stress induced gene expression drives transient DNA methylation changes at adjacent repetitive elements, Elife. 4 (2015). doi:10.7554/eLife.09343.
[18] M.J. Rowley, M.H. Rothi, G. Böhmdorfer, J. Kuciński, A.T. Wierzbicki, Long-range control of gene expression via RNA-directed DNA methylation, PLoS Genet. 13 (2017) e1006749.
[19] F. Johannes, E. Porcher, F.K. Teixeira, V. Saliba-Colombani, M. Simon, N. Agier, A. Bulski, J. Albuisson, F. Heredia, P. Audigier, D. Bouchez, C. Dillmann, P. Guerche, F. Hospital, V. Colot, Assessing the impact of transgenerational epigenetic variation on complex traits, PLoS Genet. 5 (2009) e1000530.
[20] S. Cortijo, R. Wardenaar, M. Colomé-Tatché, A. Gilly, M. Etcheverry, K. Labadie, E. Caillieux, F. Hospital, J.-M. Aury, P. Wincker, F. Roudier, R.C. Jansen, V. Colot, F. Johannes, Mapping the epigenetic basis of complex traits, Science. 343 (2014) 1145–1148.
[21] T.-N. Le, U. Schumann, N.A. Smith, S. Tiwari, P.C.K. Au, Q.-H. Zhu, J.M. Taylor, K. Kazan, D.J. Llewellyn, R. Zhang, E.S. Dennis, M.-B. Wang, DNA demethylases target promoter transposable elements to positively regulate stress responsive genes in Arabidopsis, Genome Biol. 15 (2014) 458.
[22] A. Wibowo, C. Becker, G. Marconi, J. Durr, J. Price, J. Hagmann, R. Papareddy, H. Putra, J. Kageyama, J. Becker, D. Weigel, J. Gutierrez-Marcos, Hyperosmotic stress memory in Arabidopsis is mediated by distinct epigenetically labile sites in the genome and is restricted in the male germline by DNA glycosylase activity, Elife. 5 (2016). doi:10.7554/eLife.13546.
[23] A. Boyko, T. Blevins, Y. Yao, A. Golubov, A. Bilichak, Y. Ilnytskyy, J. Hollander, F. Meins, I. Kovalchuk, Transgenerational Adaptation of Arabidopsis to Stress Requires DNA Methylation and the Function of Dicer-Like Proteins, (2010). doi:10.1371/journal.pone.0009514.
[24] E.J. Finnegan, W.J. Peacock, E.S. Dennis, Reduced DNA methylation in Arabidopsis thaliana results in abnormal plant development, Proc. Natl. Acad. Sci. U. S. A. 93 (1996)

8449–8454.
[25] H. Stroud, T. Do, J. Du, X. Zhong, S. Feng, L. Johnson, D.J. Patel, S.E. Jacobsen, Non-CG methylation patterns shape the epigenetic landscape in Arabidopsis, Nat. Struct. Mol. Biol. 21 (2014) 64–72.
[26] B.P. Williams, M. Gehring, Stable transgenerational epigenetic inheritance requires a DNA methylation-sensing circuit, Nat. Commun. 8 (2017) 2124.
[27] J. Reinders, B.B.H. Wulff, M. Mirouze, A. Marí-Ordóñez, M. Dapp, W. Rozhon, E. Bucher, G. Theiler, J. Paszkowski, Compromised stability of DNA methylation and transposon immobilization in mosaic Arabidopsis epigenomes, Genes Dev. 23 (2009) 939–950.
[28] M. Ong-Abdullah, J.M. Ordway, N. Jiang, S.-E. Ooi, S.-Y. Kok, N. Sarpan, N. Azimi, A.T. Hashim, Z. Ishak, S.K. Rosli, F.A. Malike, N.A.A. Bakar, M. Marjuni, N. Abdullah, Z. Yaakub, M.D. Amiruddin, R. Nookiah, R. Singh, E.-T.L. Low, K.-L. Chan, N. Azizi, S.W. Smith, B. Bacher, M.A. Budiman, A. Van Brunt, C. Wischmeyer, M. Beil, M. Hogan, N. Lakey, C.-C. Lim, X. Arulandoo, C.-K. Wong, C.-N. Choo, W.-C. Wong, Y.-Y. Kwan, S.S.R.S. Alwee, R. Sambanthamurthi, R.A. Martienssen, Loss of Karma transposon methylation underlies the mantled somaclonal variant of oil palm, Nature. 525 (2015) 533–537.
[29] L. He, W. Wu, G. Zinta, L. Yang, D. Wang, R. Liu, H. Zhang, Z. Zheng, H. Huang, Q. Zhang, J.-K. Zhu, A naturally occurring epiallele associates with leaf senescence and local climate adaptation in Arabidopsis accessions, Nat. Commun. 9 (2018) 460.
[30] D.R. Ganguly, P.A. Crisp, S.R. Eichten, B.J. Pogson, Maintenance of pre-existing DNA methylation states through recurring excess-light stress, Plant Cell Environ. 41 (2018) 1657–1672.
[31] S. Karpinski, Systemic Signaling and Acclimation in Response to Excess Excitation Energy in Arabidopsis, Science. 284 (1999) 654–657.
[32] J.B. Rossel, P.B. Wilson, D. Hussain, N.S. Woo, M.J. Gordon, O.P. Mewett, K.A. Howell, J. Whelan, K. Kazan, B.J. Pogson, Systemic and intracellular responses to photooxidative stress in Arabidopsis, Plant Cell. 19 (2007) 4091–4110.
[33] M.J. Gordon, M. Carmody, V. Albrecht, B. Pogson, Systemic and Local Responses to Repeated HL Stress-Induced Retrograde Signaling in Arabidopsis, Front. Plant Sci. 3 (2012) 303.
[34] M. Iwasaki, J. Paszkowski, Identification of genes preventing transgenerational transmission of stress-induced epigenetic states, Proc. Natl. Acad. Sci. U. S. A. 111 (2014) 8547–8552.
[35] T. Ito, Y. Tarutani, T.K. To, M. Kassam, E. Duvernois-Berthet, S. Cortijo, K. Takashima, H. Saze, A. Toyoda, A. Fujiyama, V. Colot, T. Kakutani, Genome-wide negative feedback drives transgenerational DNA methylation dynamics in Arabidopsis, PLoS Genet. 11 (2015) e1005154.
[36] I.R. Henderson, S.E. Jacobsen, Tandem repeats upstream of the Arabidopsis endogene SDC recruit non-CG DNA methylation and initiate siRNA spreading, Genes Dev. 22 (2008) 1597–1606.
[37] A. Khan, A. Garbelli, S. Grossi, A. Florentin, G. Batelli, T. Acuna, G. Zolla, Y. Kaye, L.K. Paul, J.-K. Zhu, G. Maga, G. Grafi, S. Barak, The Arabidopsis STRESS RESPONSE SUPPRESSOR DEAD-box RNA helicases are nucleolar- and chromocenter-localized proteins that undergo stress-mediated relocalization and are involved in epigenetic gene silencing, Plant J. 79 (2014) 28–43.
[38] H. Stroud, M.V.C. Greenberg, S. Feng, Y.V. Bernatavichute, S.E. Jacobsen, Comprehensive Analysis of Silencing Mutants Reveals Complex Regulation of the Arabidopsis Methylome, Cell. 161 (2015) 1697–1698.
[39] P. Kant, S. Kant, M. Gordon, R. Shaked, S. Barak, STRESS RESPONSE SUPPRESSOR1 and STRESS RESPONSE SUPPRESSOR2, two DEAD-box RNA helicases that attenuate

Arabidopsis responses to multiple abiotic stresses, Plant Physiol. 145 (2007) 814–830.
[40] K.K. Niyogi, C. Shih, W. Soon Chow, B.J. Pogson, D. DellaPenna, O. Björkman, 10.1023/A:1010661102365, Photosynthesis Research. 67 (2001) 139–145. doi:10.1023/A:1010661102365.
[41] H.-S. Jung, K.K. Niyogi, Quantitative genetic analysis of thermal dissipation in Arabidopsis, Plant Physiol. 150 (2009) 977–986.
[42] N. Suzuki, G. Miller, C. Salazar, H.A. Mondal, E. Shulaev, D.F. Cortes, J.L. Shuman, X. Luo, J. Shah, K. Schlauch, V. Shulaev, R. Mittler, Temporal-spatial interaction between reactive oxygen species and abscisic acid regulates rapid systemic acclimation in plants, Plant Cell. 25 (2013) 3553–3569.
[43] M. Carmody, P.A. Crisp, S. d'Alessandro, D. Ganguly, M. Gordon, M. Havaux, V. Albrecht-Borth, B.J. Pogson, Uncoupling High Light Responses from Singlet Oxygen Retrograde Signaling and Spatial-Temporal Systemic Acquired Acclimation, Plant Physiol. 171 (2016) 1734–1749.
[44] I. Gadjev, S. Vanderauwera, T.S. Gechev, C. Laloi, I.N. Minkov, V. Shulaev, K. Apel, D. Inzé, R. Mittler, F. Van Breusegem, Transcriptomic footprints disclose specificity of reactive oxygen species signaling in Arabidopsis, Plant Physiol. 141 (2006) 436–445.
[45] F. Blanco, P. Salinas, N.M. Cecchini, X. Jordana, P. Van Hummelen, M.E. Alvarez, L. Holuigue, Early genomic responses to salicylic acid in Arabidopsis, Plant Mol. Biol. 70 (2009) 79–102.
[46] F. Ramel, S. Birtic, C. Ginies, L. Soubigou-Taconnat, C. Triantaphylidès, M. Havaux, Carotenoid oxidation products are stress signals that mediate gene responses to singlet oxygen in plants, Proc. Natl. Acad. Sci. U. S. A. 109 (2012) 5535–5540.
[47] W. Pornsiriwong, G.M. Estavillo, K.X. Chan, E.E. Tee, D. Ganguly, P.A. Crisp, S.Y. Phua, C. Zhao, J. Qiu, J. Park, M.T. Yong, N. Nisar, A.K. Yadav, B. Schwessinger, J. Rathjen, C.I. Cazzonelli, P.B. Wilson, M. Gilliham, Z.-H. Chen, B.J. Pogson, A chloroplast retrograde signal, 3'-phosphoadenosine 5'-phosphate, acts as a secondary messenger in abscisic acid signaling in stomatal closure and germination, Elife. 6 (2017). doi:10.7554/eLife.23361.
[48] M. Szechyńska-Hebda, J. Kruk, M. Górecka, B. Karpińska, S. Karpiński, Evidence for light wavelength-specific photoelectrophysiological signaling and memory of excess light episodes in Arabidopsis, Plant Cell. 22 (2010) 2201–2218.
[49] F. Johannes, R.J. Schmitz, Spontaneous epimutations in plants, New Phytol. (2018). doi:10.1111/nph.15434.
[50] K.-J. Dietz, Efficient high light acclimation involves rapid processes at multiple mechanistic levels, J. Exp. Bot. 66 (2015) 2401–2414.
[51] B.J. Pogson, D. Ganguly, V. Albrecht-Borth, Insights into chloroplast biogenesis and development, Biochim. Biophys. Acta. 1847 (2015) 1017–1024.
[52] P.J. Dickinson, M. Kumar, C. Martinho, S.J. Yoo, H. Lan, G. Artavanis, V. Charoensawan, M.A. Schöttler, R. Bock, K.E. Jaeger, P.A. Wigge, Chloroplast Signaling Gates Thermotolerance in Arabidopsis, Cell Rep. 22 (2018) 1657–1665.
[53] M. Moore, M. Vogel, K. Dietz, The acclimation response to high light is initiated within seconds as indicated by upregulation of AP2/ERF transcription factor network in Arabidopsis thaliana, Plant Signal. Behav. 9 (2014) 976479.
[54] N. Suzuki, A.R. Devireddy, M.A. Inupakutika, A. Baxter, G. Miller, L. Song, E. Shulaev, R.K. Azad, V. Shulaev, R. Mittler, Ultra-fast alterations in mRNA levels uncover multiple players in light stress acclimation in plants, Plant J. 84 (2015) 760–772.
[55] L.W. Bielczynski, G. Schansker, R. Croce, Effect of Light Acclimation on the Organization of Photosystem II Super- and Sub-Complexes in Arabidopsis thaliana, Front. Plant Sci. 7 (2016) 105.
[56] C.H. Foyer, J. Neukermans, G. Queval, G. Noctor, J. Harbinson, Photosynthetic control of electron transport and the regulation of gene expression, J. Exp. Bot. 63 (2012) 1637–

1661.
[57] H. Zhu, L.-D. Zeng, X.-P. Yi, C.-L. Peng, W.-F. Zhang, W.S. Chow, The half-life of the cytochrome bf complex in leaves of pea plants after transfer from moderately-high growth light to low light, Funct. Plant Biol. 44 (2017) 351.
[58] S.A. Dwyer, W.S. Chow, W. Yamori, J.R. Evans, S. Kaines, M.R. Badger, S. von Caemmerer, Antisense reductions in the PsbO protein of photosystem II leads to decreased quantum yield but similar maximal photosynthetic rates, J. Exp. Bot. 63 (2012) 4781–4795.
[59] P.A. Crisp, D.R. Ganguly, A.B. Smith, K.D. Murray, G.M. Estavillo, I. Searle, E. Ford, O. Bogdanović, R. Lister, J.O. Borevitz, S.R. Eichten, B.J. Pogson, Rapid Recovery Gene Downregulation during Excess-Light Stress and Recovery in Arabidopsis, Plant Cell. 29 (2017) 1836–1863.
[60] P.J. Gollan, Y. Lima-Melo, A. Tiwari, M. Tikkanen, E.-M. Aro, Interaction between photosynthetic electron transport and chloroplast sinks triggers protection and signalling important for plant productivity, Philos. Trans. R. Soc. Lond. B Biol. Sci. 372 (2017). doi:10.1098/rstb.2016.0390.
[61] N.R. Baker, Chlorophyll fluorescence: a probe of photosynthesis in vivo, Annu. Rev. Plant Biol. 59 (2008) 89–113.
[62] L. Hendrickson, R.T. Furbank, W.S. Chow, A simple alternative approach to assessing the fate of absorbed light energy using chlorophyll fluorescence, Photosynth. Res. 82 (2004) 73–81.
[63] D.M. Kramer, G. Johnson, O. Kiirats, G.E. Edwards, New Fluorescence Parameters for the Determination of QARedox State and Excitation Energy Fluxes, Photosynth. Res. 79 (2004) 209–218.
[64] F. Krueger, S.R. Andrews, Bismark: a flexible aligner and methylation caller for Bisulfite-Seq applications, Bioinformatics. 27 (2011) 1571–1572.
[65] B. Langmead, S.L. Salzberg, Fast gapped-read alignment with Bowtie 2, Nat. Methods. 9 (2012) 357–359.
[66] M.D. Schultz, R.J. Schmitz, J.R. Ecker, “Leveling” the playing field for analyses of single-base resolution DNA methylomes, Trends Genet. 28 (2012) 583–585.
[67] A.R. Quinlan, I.M. Hall, BEDTools: a flexible suite of utilities for comparing genomic features, Bioinformatics. 26 (2010) 841–842.
[68] H. Feng, K.N. Conneely, H. Wu, A Bayesian hierarchical model to detect differentially methylated loci from single nucleotide resolution sequencing data, Nucleic Acids Res. 42 (2014) e69.
[69] H. Wu, T. Xu, H. Feng, L. Chen, B. Li, B. Yao, Z. Qin, P. Jin, K.N. Conneely, Detection of differentially methylated regions from whole-genome bisulfite sequencing data without replicates, Nucleic Acids Res. 43 (2015) e141.
[70] C.-Y. Cheng, V. Krishnakumar, A.P. Chan, F. Thibaud-Nissen, S. Schobel, C.D. Town, Araport11: a complete reannotation of the Arabidopsis thaliana reference genome, Plant J. 89 (2017) 789–804.
[71] R.S. Allen, J. Li, M.M. Alonso-Peral, R.G. White, F. Gubler, A.A. Millar, MicroR159 regulation of most conserved targets in Arabidopsis has negligible phenotypic effects, Silence. 1 (2010) 18.
[72] Y. Liao, G.K. Smyth, W. Shi, The Subread aligner: fast, accurate and scalable read mapping by seed-and-vote, Nucleic Acids Res. 41 (2013) e108.
[73] Y. Chen, A.T.L. Lun, G.K. Smyth, From reads to genes to pathways: differential expression analysis of RNA-Seq experiments using Rsubread and the edgeR quasi-likelihood pipeline, F1000Res. 5 (2016) 1438.
[74] H. Mi, A. Muruganujan, J.T. Casagrande, P.D. Thomas, Large-scale gene function analysis with the PANTHER classification system, Nat. Protoc. 8 (2013) 1551–1566.

[75] D. Bates, M. Mächler, B. Bolker, S. Walker, Fitting Linear Mixed-Effects Models Using lme4, J. Stat. Softw. 67 (2015). doi:10.18637/jss.v067.i01.
[76] J.S. Lefcheck, piecewiseSEM : Piecewise structural equation modelling in r for ecology, evolution, and systematics, Methods Ecol. Evol. 7 (2016) 573–579.

A Propotion methylated cytosines along chromosome 1

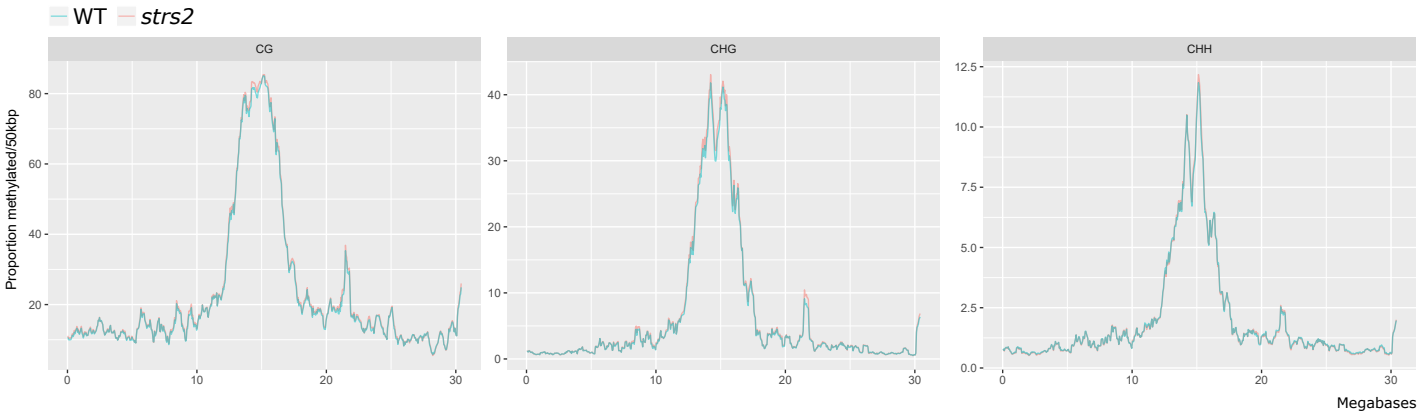

B *strs2* DMR frequency

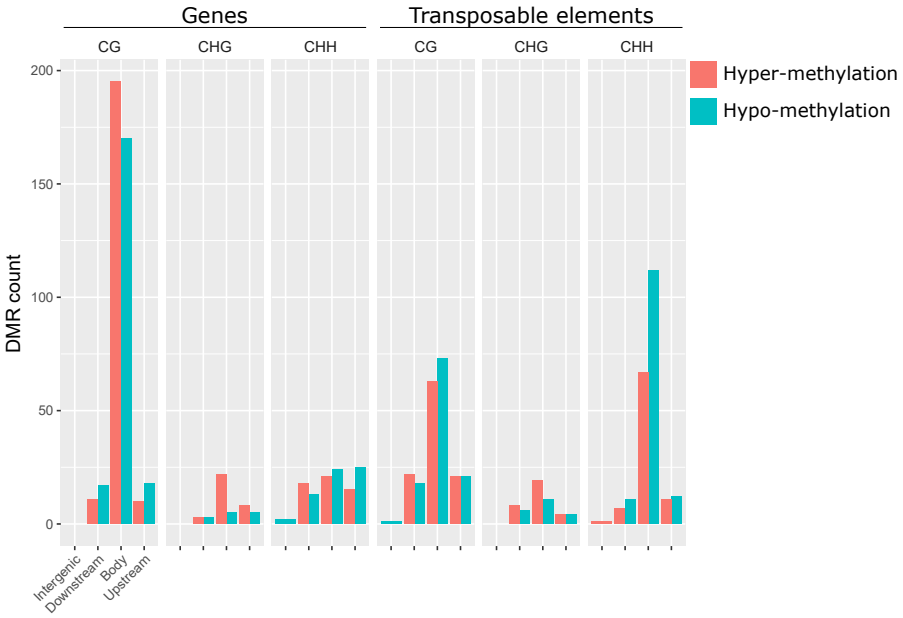

Figure 1 Subtle methylome perturbation in *strs2*

A Mean weighted methylation levels, binned into 50 kbp rolling windows, along Arabidopsis chromosome 1 for WT and *strs2*.

B DMR frequency in *strs2* grouped by genomic location relative to annotated genes or transposable elements. DMRs were classified as either occurring directly within (body), < 1 kbp away from the 5` (upstream) or 3`end of (downstream), or > 1 kbp (intergenic) away from genomic features.

A Phenotypes of DNA methylation mutants throughout development

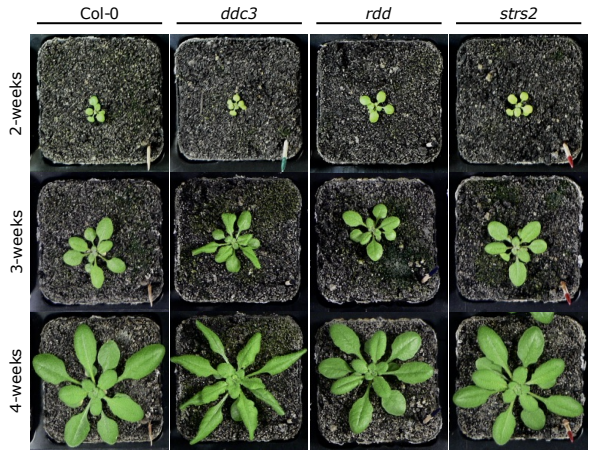

B Leaf number and plant area across development of DNA methylation mutants

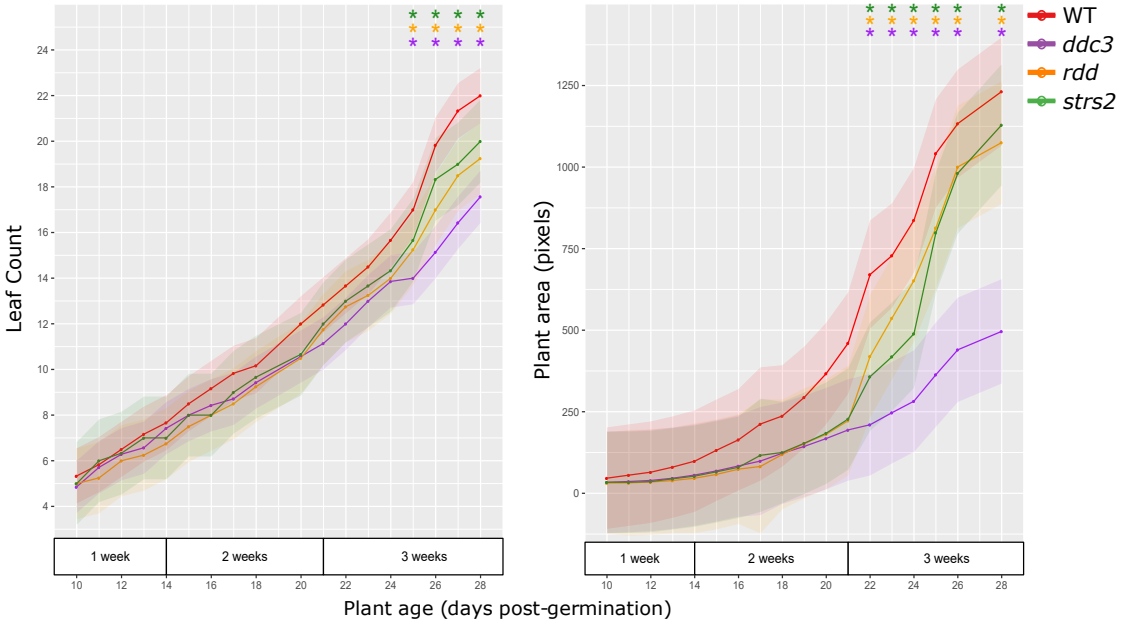

C Basal PSII performance in 3-week old DNA methylation mutants

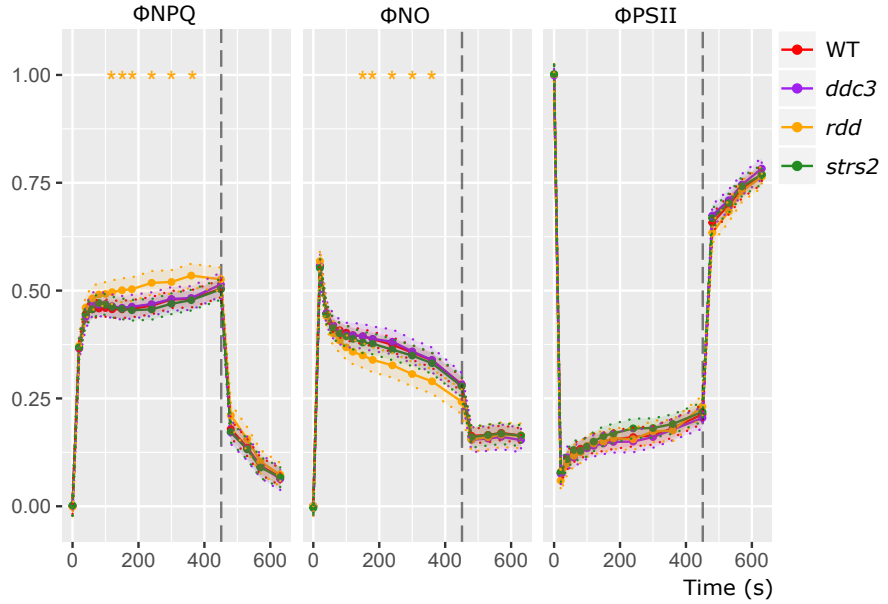

Figure 2 DNA methylation mutant development and basal PSII function
A Representative morphology of WT, *ddc3*, *rdd*, and *strs2* from 2-4 weeks of age.
B Leaf number (left) and plant area (right) in 10-day old WT (red, n=8), *ddc3* (purple, n=8), *rdd* (orange, n=8), and *strs2* (green, n=8) seedlings, monitored for 20 days until 4-weeks of age.
C Measures of PSII performance in 3-week old WT (red, n=65), *ddc3* (purple, n=10), *rdd* (orange, n=10), *strs2* (green, n=15) plants grown under standard conditions.
Points denote estimated marginal means based on a fitted linear mixed-effect model for each genotype. Bars and shaded regions denote 95% confidence intervals; * indicates statistical significance (adjusted p-value<0.05) from WT.

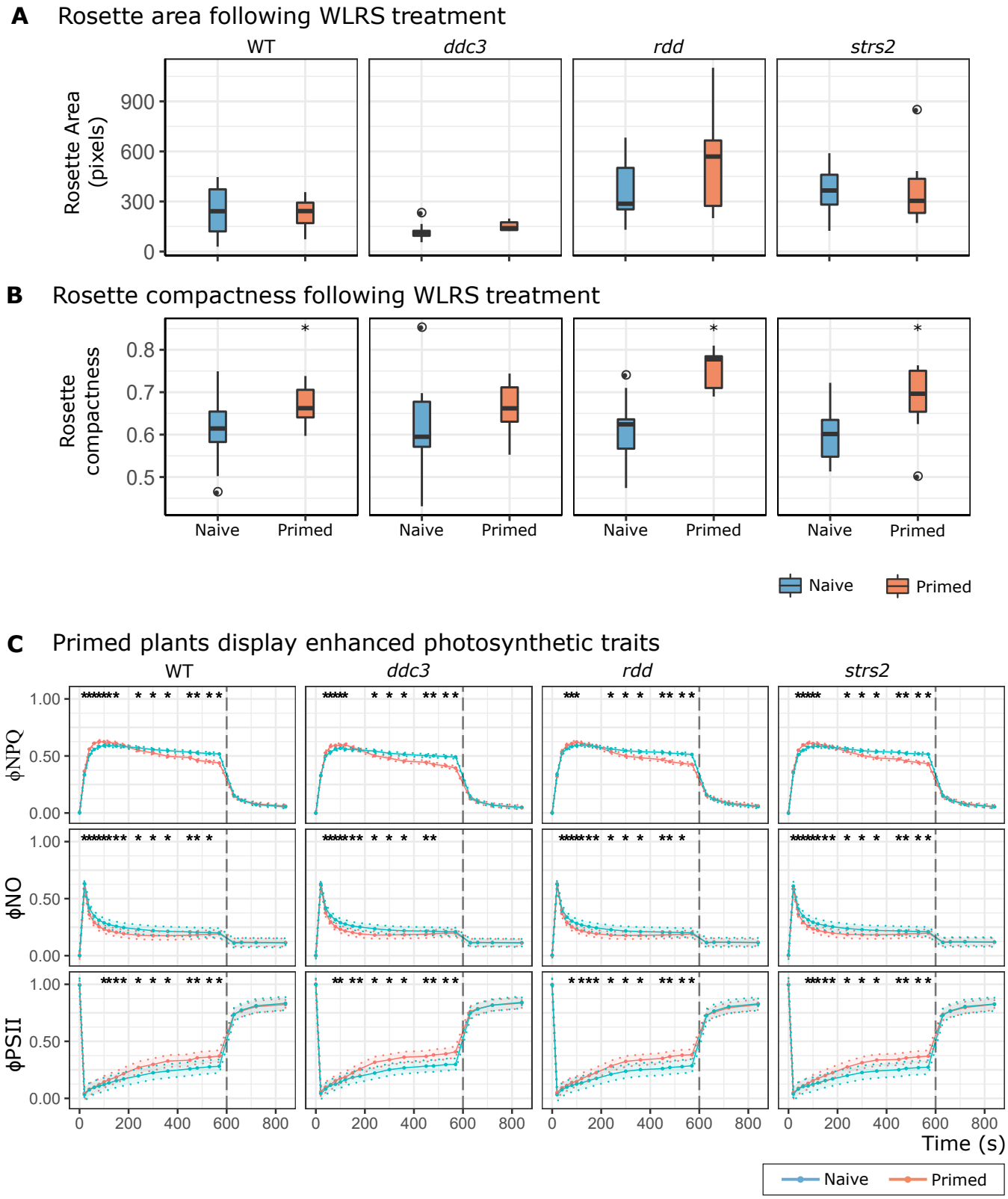

Figure 3 DNA methylation mutants are primed by recurring EL

A-B Boxplots of rosette area and compactness measured in all genotypes either exposed to recurring EL (primed, n=12-15) or not (naive, 21-23). * denotes statistical significance determined using independent Student's t-tests for each genotype (adjusted p-value < 0.05).

C PSII performance traits in naive (WT n=22; *ddc3* n=16, *rdd* n=21, *strs2* n=23) and primed (WT n=16; *ddc3* n=13, *rdd* n=12, *strs2* n=15) plants for all genotypes. Points denote estimated marginal means based on a fitted linear mixed-effect model for each genotype. Bars and shading denote 95% confidence intervals; * indicates statistical significance (adjusted p-value < 0.05) from WT.

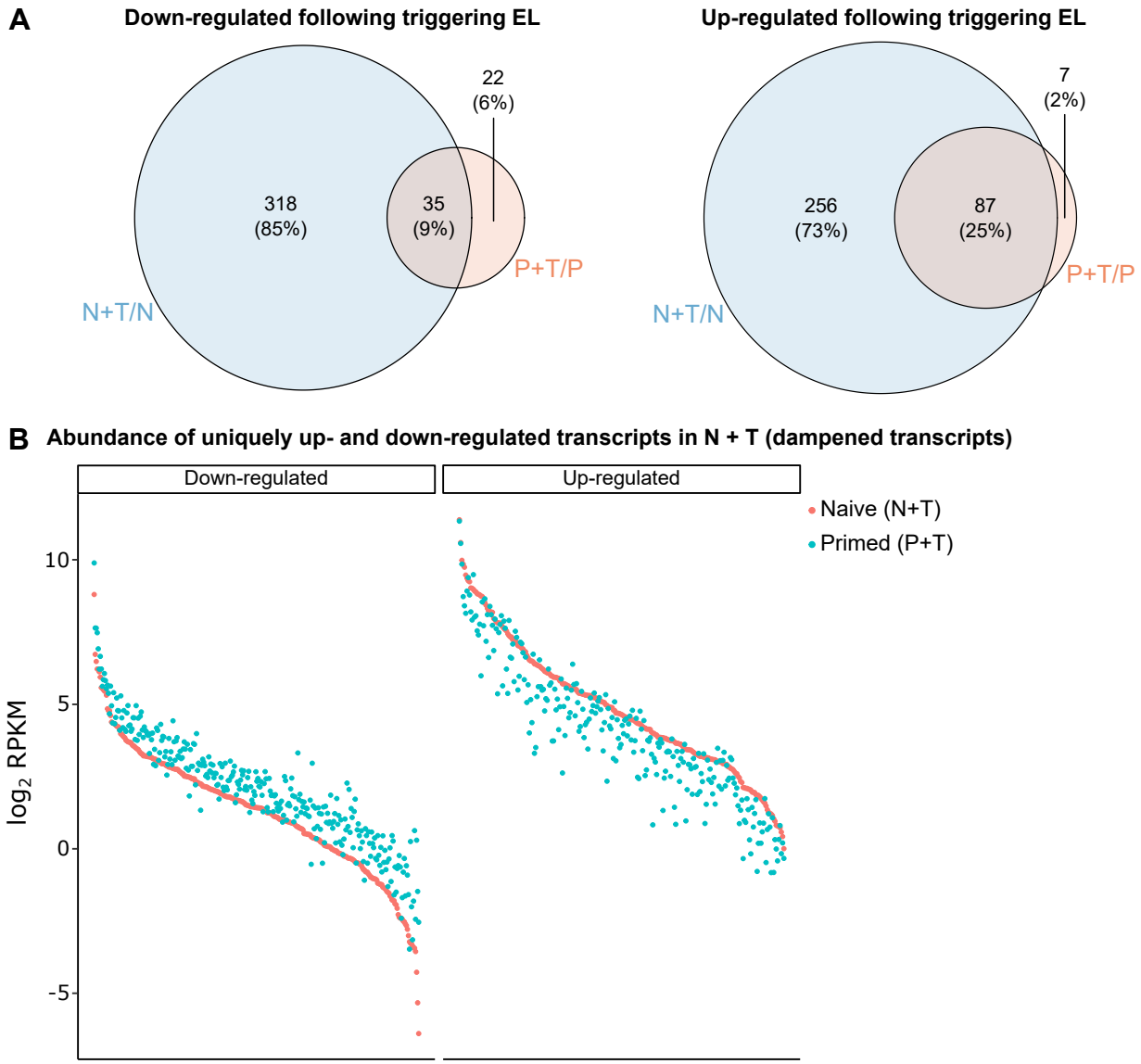

Figure 4 Transcriptional 'dampening' evident in EL primed plants
A Overlap between up- and down-regulated transcripts in naive and primed plants in response to an additional triggering EL treatment.
B Transcript abundance (log_2 RPKM) of uniquely up- (left) and down-regulated (right) transcripts, in N+T plants, for both N+T and P+T plants.

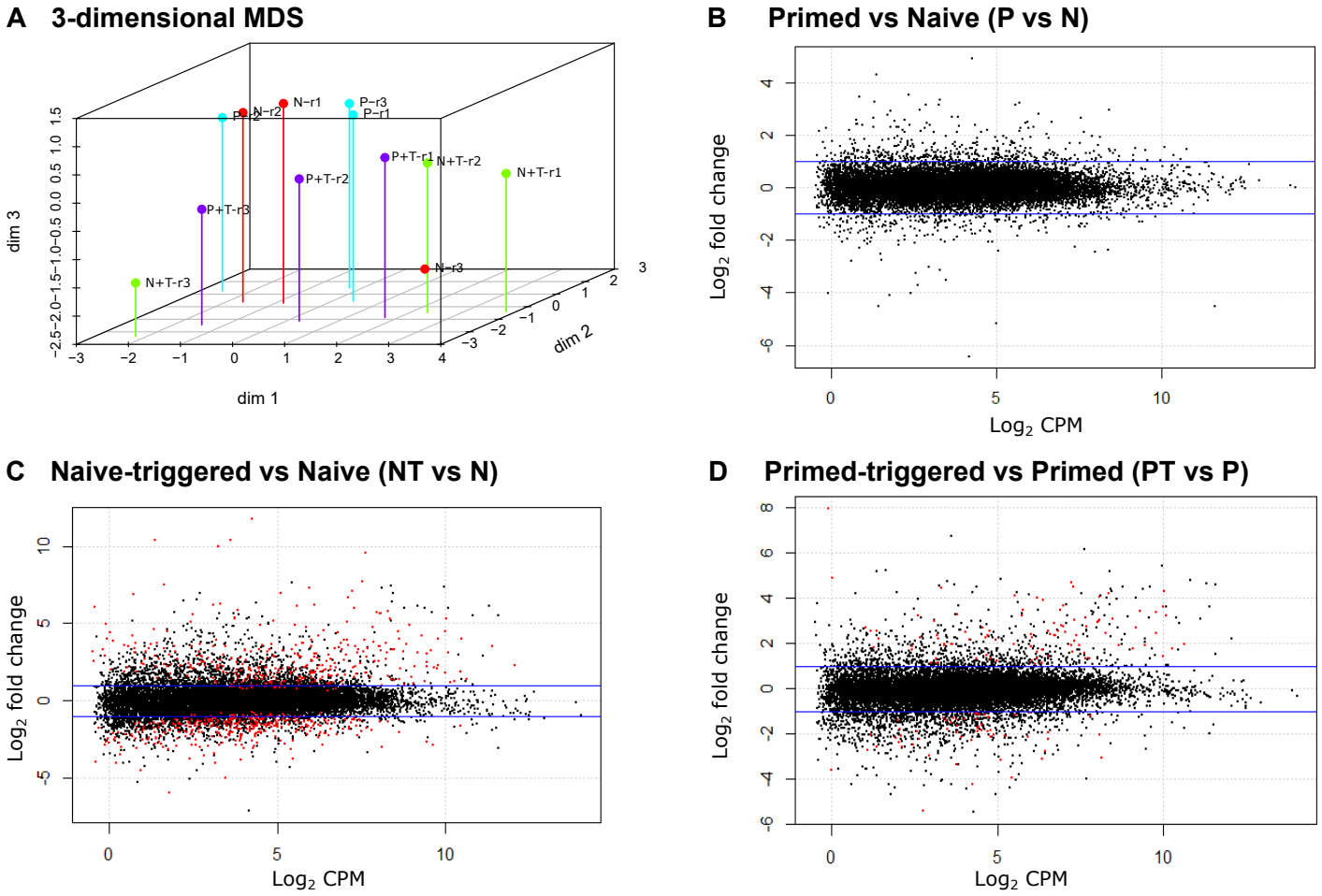

Figure S1 Exploratory transcriptome analysis of naive and primed plants
A Multi-dimensional scaling plot of all samples where distance reflects the typical $\log_2$ fold change between samples. **B-D** Mean-difference plots for **B** primed versus naive (P vs N) libraries, **C** naive-triggered versus naive (NT vs N) libraries, and **D** primed-triggered versus primed (PT vs P) libraries with smearing of low abundance transcripts. Each dot represents a transcript plotted by its average abundance ($\log_2$ CPM) against the $\log_2$ fold change from the specified comparison. Red dots indicate differentially expressed transcripts as determined by quasi-likelihood F-tests (FDR < 0.05). Blue lines denote 2-fold change.